

Optimization of melting and solidification processes of PCM: Application to Integrated Collector Storage Solar Water Heaters (ICSSWH)

A. Allouhi ^{*(a)}, A. Ait Msaad ^(a), M. Benzakour Amine ^(b), R. Saidur ^(c,d), M. Mahdaoui ^(e), T. Kousksou ^(f), **A.K. Pandey** ^(c), A. Jamil ^(a), N. Moujibi ^(a), A. Benbassou ^(a)

- ^(a) Ecole Supérieure de Technologie de Fès, U.S.M.B.A, Route d'Imouzzar, BP 2427, Fez, Morocco
- ^(b) Faculté des Sciences et Techniques de Fès, U.S.M.B.A, Route d'Imouzzar, BP 2202, Fez, Morocco
- ^(c) Research Centre for Nano-Materials and Energy Technology (RCNMET), School of Science and Technology, Sunway University, No. 5, Jalan Universiti, Bandar Sunway, Petaling Jaya, 47500 Selangor Darul Ehsan, Malaysia
- ^(d) Department of Engineering, Lancaster University, Lancaster, LA1 4YW, UK
- ^(e) Faculté des Sciences et Techniques, U.A.E, Tangier, BP 416, Morocco
- ^(f) Laboratoire des Sciences de l'Ingénieur Appliquées à la Mécanique et au Génie Electrique (SIAME), Université de Pau et des Pays de l'Adour – IFR – A. Jules Ferry, 64000 Pau, France

Abstract

This work presents a detailed analysis of an improved Integrated Collector Storage Solar Water Heater (ICSSWH). This type of device is well suited for rural areas of Morocco because of its low cost, simplicity and compact structure. The innovation targeted in this system lies in the integration of a latent storage system by using a layer of phase change materials (PCM) in its lower part. Indeed, this integration is likely to increase the thermal energy delivered to the user during the night. The overall performance of the system depends on external climate data, type of PCM used and its mass, and flow rate of water. N-eicosane is considered as PCM in this application while hourly weather data corresponding to the city ER-RACHIDIA is used for the analysis. A detailed 2-D transient simulation has been established to optimize the system performance by studying the effect of different design variables and operating conditions. A deep analysis was also made to understand the PCM melting and solidification processes for a better exploitation of this storage technique. Optimized results are obtained when a mass flow rate of 0.0015 kg/s is used with a PCM thickness of 0.01 m and a set temperature of 313 K.

Keywords:

ICSSWH; PCM; Melting/ Solidification; Thermal energy; Rural zones

Nomenclature

P : pressure (Pa)

T : temperature (K)

t : time (s)

\vec{g} : Acceleration of gravity vector (m/s^2)

V : fluid velocity vector (m/s)

H : specific enthalpy (J/kg)

C_p : specific heat capacity (J/kg K)

h_{ref} : enthalpy at reference temperature (J/kg)

L : latent heat of PCM (J/kg)

f : liquid fraction (%)

r : reduction in missed thermal energy (%)

Q_{missed} : missed thermal energy (kWh)

T_{wi} : water inlet temperature (K)

T_{wo} : water outlet temperatures (K)

T_{set} : Set temperature (K)

C_w : specific heat of water (J/kg K)

\dot{m} : mass flow rate (kg/s)

Greek letters

μ : dynamic viscosity (kg/m s)

ρ : density (kg/m^3)

Abbreviation

ICSSWH : Integrated Collector Storage Solar Water Heaters

PCM : phase change materials

SWH: Solar water heaters

1. Introduction

Either thermal or electrical energy is crucial for the social development in rural areas [1]. With the currently unsustainable energy system, tremendous efforts are still needed to ensure equitably energy demand for the future generations by providing clean, secure and affordable alternatives. Solar energy has the most important potential to fulfill the increasing energy requirements [2]. Both thermal and photovoltaic conversions of solar energy have been a focal research point over the last years academically and industrially. The main aim of the deployed efforts is to improve performance and reduce costs [3-4]. Solar water heaters (SWH) have gained particular interest as a promising option for satisfying hot water requirements worldwide [5]. Currently, various SWH designs are available in the market with increasingly decreasing costs [6]. Globally, a total installed capacity of 410.2 GW_{th} was reached, which is equivalent to 586 million square meters of collector surface [7]. In urban areas, passive thermo-syphonic SWH are often preferred for hot water production in the residential sectors [8]. In turn, active SWH using circulating pumps are more adapted to large commercial and industrial applications [9]. For low income communities residing in rural areas, integrated collector storage solar water heater (ICSSWH) can meet a considerable portion of the hot water demand [10]. These systems are gaining popularity as they present higher reliability, simpler designs and lower prices. Accordingly, they can be more adapted to rural regions possessing more potential solar energy sources [11]. The main drawback of these systems lies in their high heat losses during night periods. Extensive research works were conducted to overcome this problem and several modified designs were proposed. Examining the open literature, one can remark that the main research contributions concerned improved practices for efficient energy collection and heat storage [12-14]. Earlier, triangular and rectangular ICSSWHs with transparent insulation were introduced in many studies [15-16]. These studies focused on the optimization of the thickness of the transparent insulation for the best performance of the system. An immersed tube heat exchanger, inside a flat plate ICSSWH was examined by Gertzos et al. [17] to intensify the heat transfer from the stored water to the service water. Tripanagnostopoulos and Souliotis [18] presented a cylindrical horizontal water storage tank placed inside the stationary truncated asymmetric CPC reflector. Authors compared the new configuration with a symmetric CPC reflector and with a typical thermosiphonic unit. It was pointed out that the proposed design demonstrated better preservation of hot water temperature during the night. Garnier et al. [19] studied and optimized a rectangular-shaped box assembling the solar collector and storage tank into a single unit, longitudinal stratification of temperature within the collector was modeled

and the system efficiency was discussed. Kumar and Rosen [20] have introduced a corrugated absorber surface over plane surface in the ICSSWH. Without making significant increase in the system price, this configuration has allowed significant efficiency improvement at higher outlet temperature. Further recent investigations regarding improving thermal efficiency and storage capacity of ICSSWH can be found in [21-25].

Latent heat thermal energy storage is one of the most efficient ways to store thermal energy received from sun [26-28]. Many investigations dealt with this topic especially in separated solar water heaters by incorporating Phase Change Materials (PCMs) in hot storage tanks. In this regards various designs have been proposed. Comprehensive reviews of the most relevant designs and improvement can be found in recent papers [29-30]. The use PCM in ICSSWH seems to be an interesting opportunity for extending operational period of hot water production [31-34]. Eames and Griffiths [35] studied heat collection and release of heat in the rectangular ICSSWH filled with water and different concentrations of PCM slurries of a 65 °C phase change temperature. The analysis showed that storing energy at a higher temperature in the PCM slurry permitted greater performances. Reddy [36] studied an ICSSWH comprising a double rectangular enclosure incorporating paraffin wax on its top surface while water flows in the bottom. The analysis showed that the system utilizing 9 fins led to a maximum water temperature and minimum heat losses to the ambient. The potential of using PCM in an ICSSWH with a cylindrical water storage tank fixed in a compound parabolic concentrating reflector has been examined using 3D CFD simulations by Chaabane et al. [37]. Myristic acid and RT42-graphite were considered as tested PCMs and three radiuses of PCM layers were analyzed. Both PCMs affected positively heat preservation of the system with a remarkable superiority of myristic acid. Recently, Al-Kayiem and Li [38] investigated experimentally a flat plate ICSSWH operating with paraffin wax as a PCM and a nanocomposite of paraffin wax with 1.0 wt% of 20-nm nano-Cu particles. Optimum inclination of the collectors was estimated to 10° for the installed system in Malaysian university. An increase of thermal efficiency by 3.5% was reported when using paraffin wax. As can be seen from the literature review, using PCMs to enhance the performance of ICSSWH is not extensively discussed compared with separated SWHs. Further simulation works are therefore required to identify best conditions of using latent heat storage for these particular systems. Selection of material, its position and how the thermal behavior of the PCM-based ICSSWH is affected by operating conditions and weather data are tremendous aspects that should be decided judiciously for a better exploitation of latent energy for maximum solar fractions.

Many authors [39-41] conducted the experimental study on the application of PCMs in solar water heaters such as Fazilati and Alemrajabi [39] experimentally investigate the effect of PCM in solar water heater. They found that energy storage density increased upto 39% and water supply more than 25% longer by using PCM as compared to without PCM. Papadimitratos et al. [40] presented a novel method of PCM encapsulation in evacuated tube collector based (ETC) based solar water heater (SWH) which uses two different PCMs viz. Trtriacontane and Erythritol. The efficiency improvements were found to be 26% and 66% for normal and stagnation mode respectively as compared to SWHs without PCM. Kılıçkap et al. [41] performed an experimental study on the encapsulation of PCM in flat plate collector based solar water heater under Elazığ climatic conditions in the months of July-November. The maximum collector efficiency with PCM was found to be 58% which was 2% higher than that of without PCM in the month of July. Therefore, in general the performance of solar collectors with PCM were found to be higher than those of solar collectors without PCM which is further confirmed by Khan et al. [42] and Pandey et al. [43] in the form of review papers.

In this paper, a 2-D numerical model is investigated to justify the benefits of using PCM in a low-cost and simple design ICSSWH to be in use by low income communities living in rural regions. Optimizing melting/solidification processes are investigated and key operating conditions are studied under real fluctuating climatic conditions. Moreover, a new performance index is introduced to assess the benefit of using PCMs compared to basic configurations in such particular solar thermal applications.

2. System design

The basic configuration of integrated collector storage solar water heater (ICSSWH) is shown in **Fig. 1 (a)**. The height of the storage unit and the area of the absorber surface are fixed at 0.08 m and 1 m², respectively. When solar radiation strikes the glass cover, the transmitted heat is transferred to the water causing a gradual increase in its temperature. The inlet water at low temperature penetrates on the line located at the left side of the collector while the heated water exits from the high right side line. The diameter of inlet and outlet pipes is 0.02 m. To suppress bottom and side heat losses, fiber-glass insulation is applied. It may also be noted that night insulation can be utilized after sunset to prevent heat losses. The improved configuration considers incorporating a layer of Phase Change Material (PCM) at the bottom side of the ICSSWH (see **Fig. 1 (b)** and **(c)**). The melting/solidification of PCM inside the rectangular cavity is studied under the fluctuating operating conditions to have insight about optimum

design variables leading to the maximum benefit of using latent heat storage techniques in such solar thermal energy systems.

3. Mathematical formulation

The studied domain consists of two parts. The first is the water inside the tank and the second is the PCM cavity. This section presents briefly the mathematical model and the governing equations describing the physical problem.

3.1. Model and grid

In this work, the commercial CFD tool Fluent was employed to investigate the numerical simulation. A quadrilateral grid was applied to construct the computational domain using Gambit software, with a total number of 29,925 cells. For all parametric studies, Reynolds number is considered <200 . An unsteady 2-D laminar incompressible model was selected to simulate the ICSSWH. At the absorber surface, a realistic and time-dependent heat flux following approximately a sinusoidal function has been introduced as user-function. It was constructed by considering global incident radiations on a tilted surface of 45° in Errachidia region (Morocco). Ambient temperatures were also generated and interpolated for three consecutive spring days. Heat losses by conduction, convection and radiation were expressed as a function of difference between ambient and absorber temperatures and an overall heat coefficient which was estimated as described by Klein [44]. The other walls (back and lateral surfaces) were supposed to be well-insulated. Moreover, a zero pressure gradient condition is used across the outlet boundary. Inlet water temperature was taken as constant in all the simulations and corresponds to 288 K.

3.2. Phase change formulation

Melting/solidification processes are described considering the enthalpy formulation. Instead of using the split-second computation of the melted surface, a parameter called the liquid fraction, measuring the ratio of the cell volume that is in liquid form, is evaluated in each cell of the domain. Governing equations can, therefore, be expressed as:

- **Continuity**

$$\frac{\partial \rho}{\partial t} + \nabla \cdot (\rho V) = 0 \quad (1)$$

- **Momentum**

$$\frac{\partial}{\partial t}(\rho V) + \nabla \cdot (\rho V) = -\nabla \cdot P + \mu \nabla^2 V + \rho g + S \quad (2)$$

- **Energy**

$$\frac{\partial}{\partial t}(\rho H) + \nabla \cdot (\rho V H) = \nabla \cdot (k \nabla T) \quad (3)$$

where ρ is the density, V is the fluid velocity vector, μ is the dynamic viscosity, P is the pressure, T is temperature, g is the gravitational acceleration, k is the thermal conductivity and H is the specific enthalpy is obtained by the following equation:

$$H = h_{ref} + \int_{T_{ref}}^T c_p dT + fL \quad (4)$$

h_{ref} denotes the enthalpy at reference temperature, c_p and L are the specific heat and the latent heat of PCM. The liquid fraction f is evaluated at each cell using the next equation:

$$\left\{ \begin{array}{ll} f = 0 & \text{if } T < T_S \\ f = 1 & \text{if } T > T_L \\ f = \frac{T - T_S}{T_L - T_S} & \text{if } T_S < T < T_L \end{array} \right. \quad (5)$$

T_S is defined as the maximum temperature at which the PCM is at solid state while T_L is defined as the minimum temperature at which it is at liquid state. The source term S figuring in the momentum equation represents the Darcy's law damping term. It can be expressed as:

$$S = \frac{C(1-f)^2}{f^3 + \varepsilon} V \quad (6)$$

C is a constant measuring the shape evaluation of the melting zone and ϵ is a very small value to avoid the zero division. For further details regarding the resolution method and phenomenon description, readers are referred to previous works [45-49]. The thermal properties of the used PCM (n-eicosane) are listed in **Table 1** [50].

3.3. Energy performance

The improved configuration of the ICSSWH using PCM has the potential to reduce the daily missed thermal energy. This relative reduction can be expressed as follows:

$$r = \frac{Q_{missed} \Big|_{without PCM} - Q_{missed} \Big|_{with PCM}}{Q_{missed} \Big|_{without PCM}} \quad (7)$$

The missed thermal energy Q_{missed} depends on the set temperature at which the water is needed and can be evaluated as:

$$Q_{missed} = \dot{m} c_w \left[\int_{t_{sr}^j}^{t_{sr}^{j+1}} ((T_{set} - T_{wi}) - (T^* - T_{wi})) dt \right] \quad (8)$$

with

$$T^* = \begin{cases} T_{wo} & \text{if } T_{wo} < T_{set} \\ T_{set} & \text{otherwise} \end{cases}$$

where t_{sr}^j and t_{sr}^{j+1} represent the sunrise of day j and day $j+1$, respectively. \dot{m} is the mass flow rate (kg/s) and T_{wi} and T_{wo} are the water inlet and outlet temperatures, respectively. T_{set} is the set temperature and c_w is the specific heat of water. It is interesting to note that the integration of Q_{missed} is carried out numerically using the trapeze method. Parametric analyses included various values of set temperatures as well.

4. Model validation

To justify the validity of the current numerical model, a comparison has been made between simulation results and experimental data reported by Gau and Viskanta's [48]. The physical

problem analysed by these authors is the melting of PCM inside a rectangular enclosure taking into account the natural convection. Geometrically, the enclosure has a width of 0.0635 m and a length of 0.0889 m. Gallium with a purity of 99.6% and a fusion temperature of 302.93 K was used in the experiments. The left and right wall temperature was fixed to 331.5 K and 301.45 K, respectively whereas the horizontal walls were insulated. Under the same conditions, simulations have been launched and the variation of the melt front with time has been predicted. A comparison between the obtained numerical results and the experimental data is illustrated in **Fig. 2**. As can be seen, the computed results are in a good agreement with the experimental data which indicates that the numerical model is valid.

5. Results and discussion

To investigate the melting/solidification processes of the PCM more realistically and study its benefit during the night period, real fluctuating climatic data in terms of incident solar radiation and ambient temperature were integrated in the simulation process. Three consecutive sunny days (with various maximum solar radiation levels) were considered to follow the daily thermal behavior of the ICSSWH considering different initial conditions. A plot of the incident solar radiation and external ambient temperatures is presented in **Fig. 3**. The maximum global solar radiation is recorded at midday with values in the range of 1050-1150 W/m². Ambient temperatures exceed 296 K during the daytime period and fall below 284 K during late hours of the night.

A significant part of the incident solar radiation penetrates through the glass cover and is absorbed by the metallic absorber plate according to the value of the transmittance-absorbance product. The upcoming energy causes an elevation of the absorber temperature. The thermal behavior of the collector absorber is shown in **Fig. 4**. During the daytime, heat is transmitted to water and then to the PCM. The melting process takes place while storing a certain amount of thermal energy. At night, the absorber gets cooled and the water temperature decreases. The PCM gets solidified and release heat which significantly increase the water temperature even during the night. Maximum absorber temperatures for the first and third days are around 340 K. A more important value of the maximum absorber temperature (364 K) is observed during the second day. Minimum temperatures of the absorber are in the range of 288-295 K.

The first set of results reports the predicted temperature at the collector outlet versus the time. The mass flow rate at the inlet pipe is fixed at 0.002 kg/s and the inlet temperature is taken as 288 K. A PCM layer is applied at the entire bottom surface as indicated in **Fig. 1 (b)**. The layer thickness was taken initially as 0.02 m.

Fig. 5 shows the hourly temperature profile in the case where no PCM is introduced (configuration C0) and when it is added as indicated in the configuration C1 (see **Fig. 1**). Starting from $t=0$ (i.e. the sunrise), the outlet water temperature increases progressively and reaches its maximum value after approximately 10 hours. Before 15 hours from the sunrise, it is clearly seen that water temperature using a layer of PCM is less important than its temperature in the basic configuration. In fact, during this phase, the PCM stores the energy originating from the hot water circulating directly above it by means of convection heat transfer. The reverse tendency is observed just after this time showing the release of heat causing an increase in the water outlet temperature. Similar behavior is approximately seen in the next days with greater energy stored and released in the second day because of the relatively high solar fluxes.

To illustrate more precisely the phase change phenomenon, the time variation of the PCM's liquid fraction (average values) is given in **Fig. 6**. The mass flow rate was varied between 0.00075-0.003 kg/s and the other operating conditions were kept constant. It is clear that, for this first configuration, the PCM does not reach a complete melting since the plotted liquid fractions are all $<65\%$. Moreover, for some flow rates, the PCM cannot be solidified completely (liquid fractions >0). This indicates that only a part of heat is stored/released which does not allow optimized utilization of this storage technique. Also, it can be seen that the melting fraction varies significantly with the change of the water flow rate.

High inlet flow rates induce lower liquid fractions during the charging process but permit a full solidification of the PCM. Alternatively, low flow rates are characterized by increased liquid fractions during the charging process but in turn do not allow a full solidification of the PCM during the discharging period.

This result can be explained by the fact that increasing water flow rates restrains the melting process since the most important part of the useful heat (upcoming from solar energy) is transferred to the circulating water and only a little amount is absorbed by the PCM. The first configuration seems to be inappropriate as the melting/solidification processes do not complete for all the tested flow rates.

Further investigation is required to understand the obtained results. Liquid fractions contours for this first configuration are displayed for different periods of the second simulation day as given in **Fig. 7**. As can be seen, in lower parts of the collector, the liquid fraction is always equal to 0 which means that the PCM in this zone does not reach its melting temperature. This can be attributed to thermal stratification due to natural convection. Hot water flows in the upper zones of the storage volume while the bottom remains at a lower temperature. This confirms the lower average liquid fractions previously presented.

An optimized configuration is proposed by adding the PCM layer only at the upper part of the collector's bottom surface as described in **Fig. 1 (c)**. This will allow a better and more rational exploitation of the heat storage technique since a greater part of the PCM is expected to melt compared to the first configuration. Simulations results of the predicted average liquid fractions for this second configuration and for three PCM thicknesses ($e=0.01$ m, $e=0.02$ m and $e=0.03$ m) are plotted in **Fig. 8**. As expected, generally, the liquid fraction evolution is characterized by more complete melting/solidification processes compared with the first configuration (C1). Furthermore, it is noticed that the PCM thickness affects significantly the melting/solidification processes. Overall, a thickness of 0.01 m causes a remarkable increase in the liquid fractions with a better solidification process. Also, low mass flow rates permit reaching higher liquid fractions by opposition to high flow rates that show generally a full solidification but partial melting processes. As can be seen, it is not easy to select the optimum variables inducing the best storage mode. However, high solar intensities (day 2) and low PCM thicknesses exhibit more complete solidification and melting processes. For low solar intensities (day 1 and day 3), other PCMs with a lower melting-temperature can be recommended for a better utilization of latent heat storage. Further numerical studies are therefore required to study the potential of other PCM candidates. Of course, an optimum selection of the PCM should be made by considering the stochastic variation of the solar incident solar radiation with respect to the concerned geographical site where the system may operate.

For the PCM used in this study and for the second simulation day, the missed thermal energy on a daily basis is evaluated for various mass flow rates, set temperatures and PCM thicknesses. The results are presented in **Table 2**. The obvious observation is that an increased set temperature engenders higher amount of missed thermal energy for all the studied cases, independently. Furthermore, the daily missed thermal energy is greatly influenced by the

operating conditions. For a better illustration of the obtained results, a graphical presentation of the reduction in the missed thermal energy when using a PCM layer is given in **Fig. 9**. It can be seen that: (i) Higher reductions in missed thermal energies are reached when the set temperature is minimized to 313 K; (ii) A PCM thickness of $e=0.01$, independently of the operating mass flow rate, generates higher reductions in the missed thermal energy; (iii) In general, a mass flow rate of 0.0015 kg/s seems to be the most convenient and can induce a reduction of the missed thermal energy up to 32% if a PCM thickness of 0.01 m is used at a set temperature of 313 K.

It is well known fact that solar radiation is intermittent in the nature and available only in the day time therefore, limitation of solar energy systems lies in the utilization when there is availability of Sun. Keeping the fact in the mind that PCMs act as a thermal energy storage by changing its phase at particular temperature, so PCMs can be used as a thermal energy storage which can be used in the absence of solar radiation. Therefore, integrating n-eicosane as a PCM which is having high latent heat 237.4 kJ/kg in real SWH system will make the system more reliable and sustainable and PCM integrated SWH system will be able to be used even in the absence of solar radiation. The investigated PCM integrated SWH system can be used for the low temperature applications viz. bathing and washing especially in the rural households of Errachidia (Morocco). The missed thermal energy can be saved up to 32% using PCM in SWH.

The extra cost incurred by using N-eicosane as a PCM in solar water heater is evaluated and presented in the **Table 3** which is calculated based on the total cost of collector/unit is USD 220 and cost of PCM/kg is USD 7.04 as per Moroccan market. From the Table 3 it can be observed that as the thickness of PCM layer is increases, the extra cost also increases due to increased amount of PCM used. Lowest extra cost is found to be for 0.01 m thickness which is also the case of optimised results. Only 14.3% will be an extra burden of cost by using the PCM while, there are several advantages of the integration of PCM in real SWH such as utilization even in the absence of solar radiation, prolonged use, sustainability, overall performance improvements and thermal energy saving.

6. Conclusion

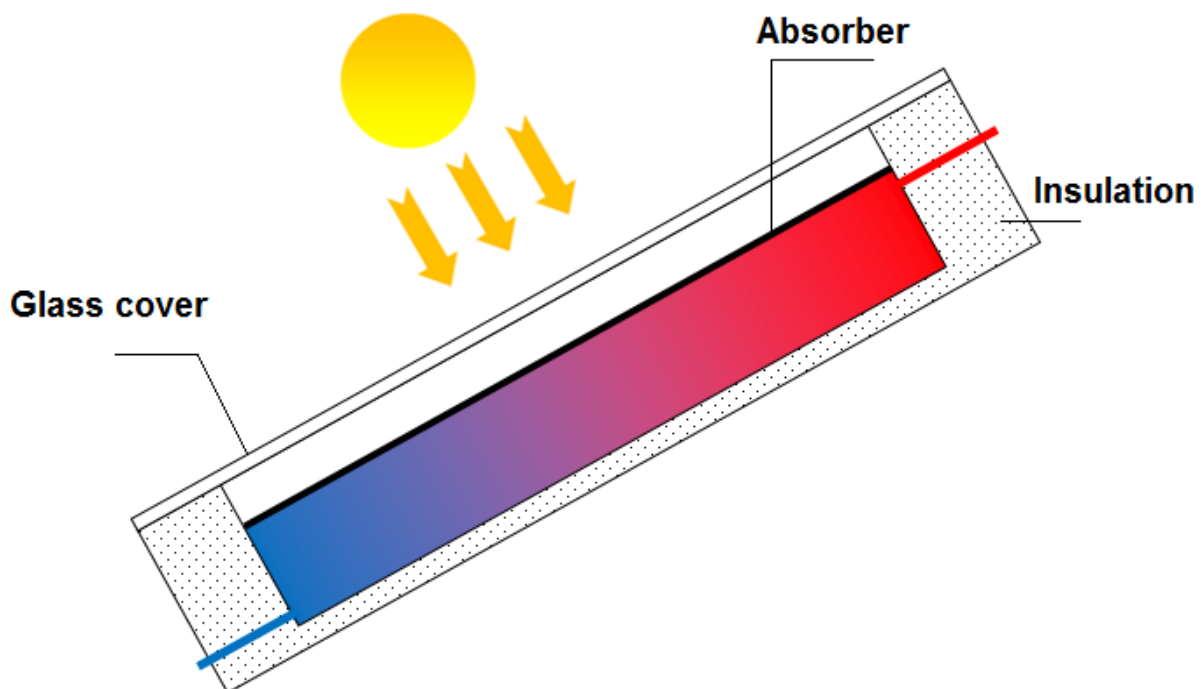
This paper investigates numerically a detailed analysis of an integrated collector storage solar water heater (ICSSWH) using a PCM layer in its lower part. Such a system can be used by rural households to fulfill hot water requirements for hygiene purposes such as bathing and washing.

The meteorological data of three typical sunny days in Errachidia (Morocco) was considered. The thermal behavior of the ICSSWH without and with PCM was presented and a parametric analysis was conducted via a detailed 2-D mathematical model. The performance of the improved system was analyzed through the assessment of missed thermal energy by considering various set temperatures, mass flow rates and PCM thicknesses. Several scenarios were discussed and the optimum operating conditions were determined. It was found that optimized results are obtained when a mass flow rate of 0.0015 kg/s is used with a PCM thickness of 0.01 m and a set temperature of 313 K. Furthermore, it was highlighted that incident solar radiation has a strong influence on the melting/solidification processes. In this sense, the test of other PCM candidates taking into account the solar energy potential of the studied region is recommended.

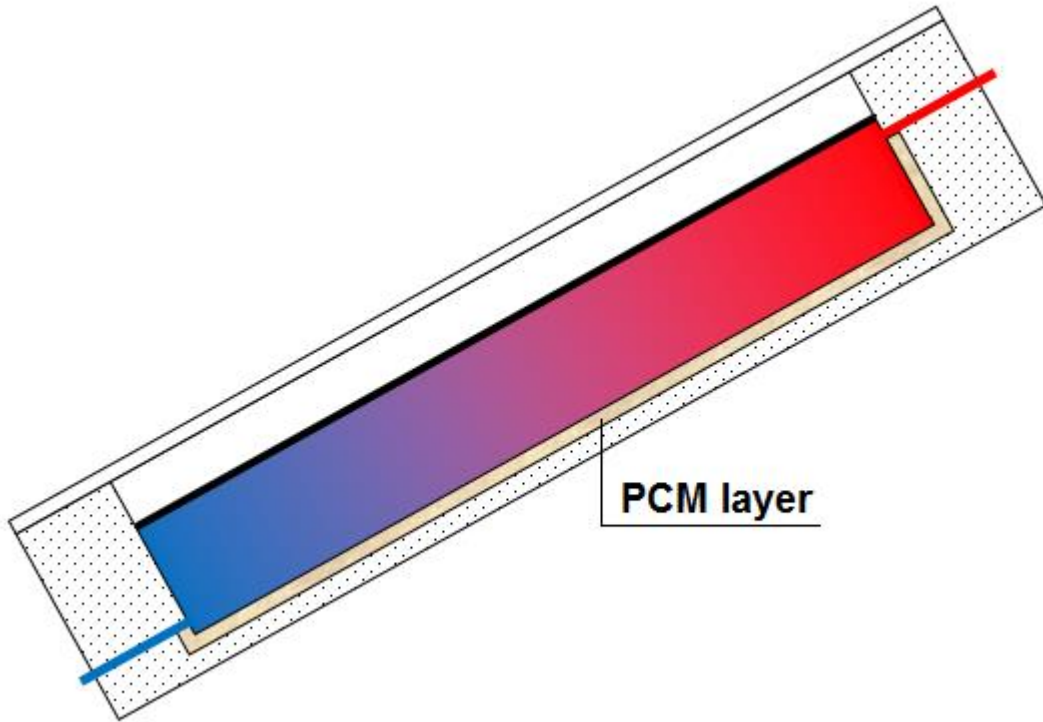
Acknowledgments

The authors acknowledge the support provided by the "Institut de Recherche en Energie Solaire et Energies Nouvelles (IRESEN)" under the project SOL'R SHEMSY.

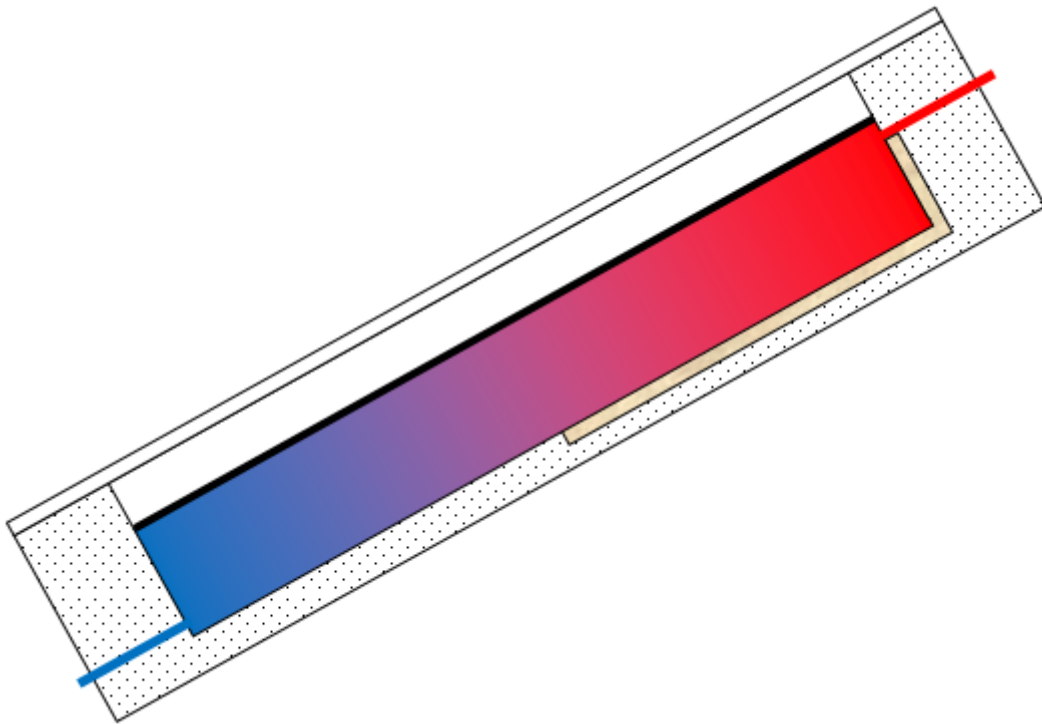
Figures list:



(a) without PCM: basic configuration (C0)



(b) with PCM: first configuration (C1)



(c) with PCM: second configuration (C2)

Fig. 1: Integrated collector storage solar water heater (various configurations)

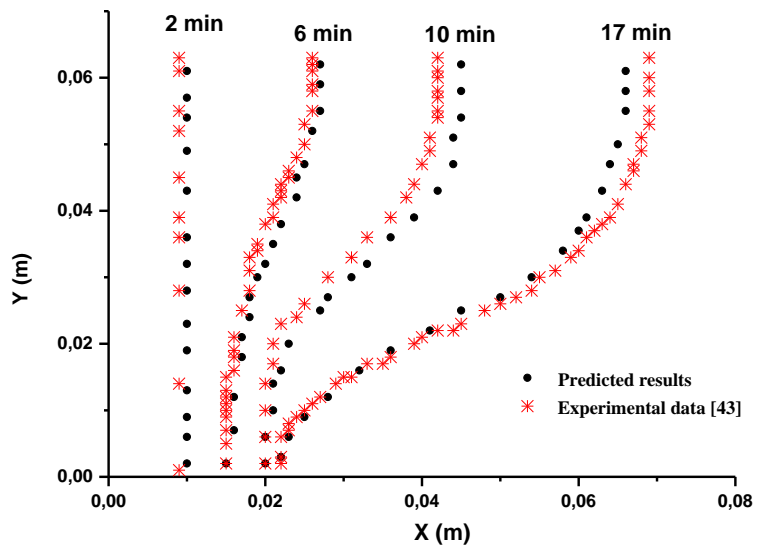
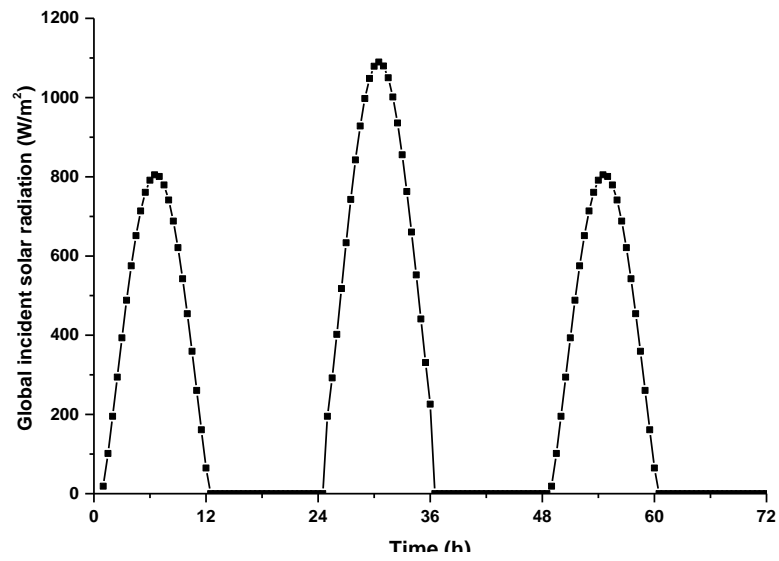
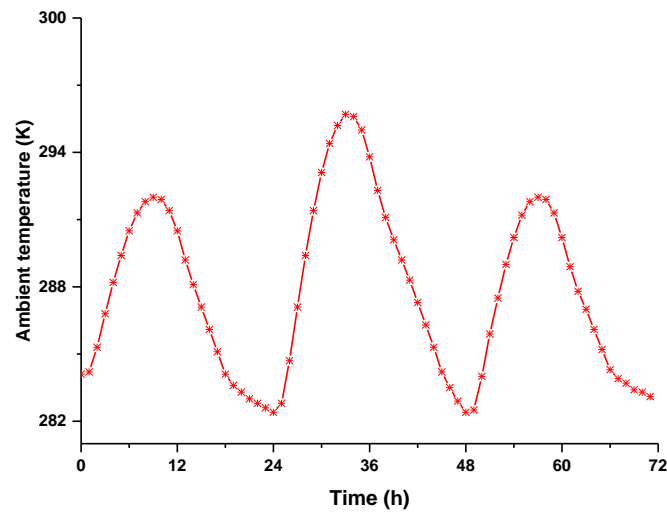


Fig. 2: Variation of the melt front with time (predicted and experimental values)



(a) Global incident solar radiation



(b) Ambient temperature

Fig. 3: Hourly climatic data used in the simulation process

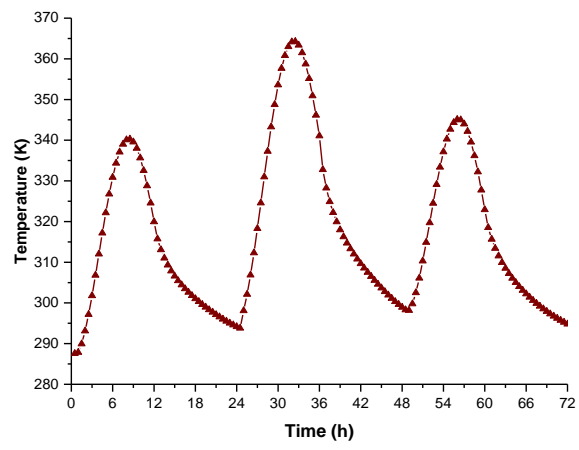


Fig. 4: Absorber temperature versus the time

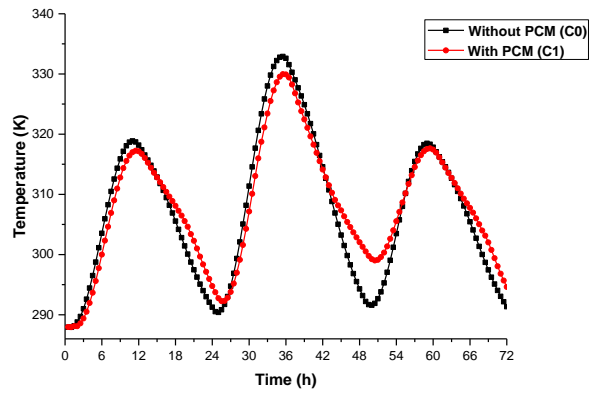


Fig. 5: Variation outlet water temperature for C0 and C1 configurations

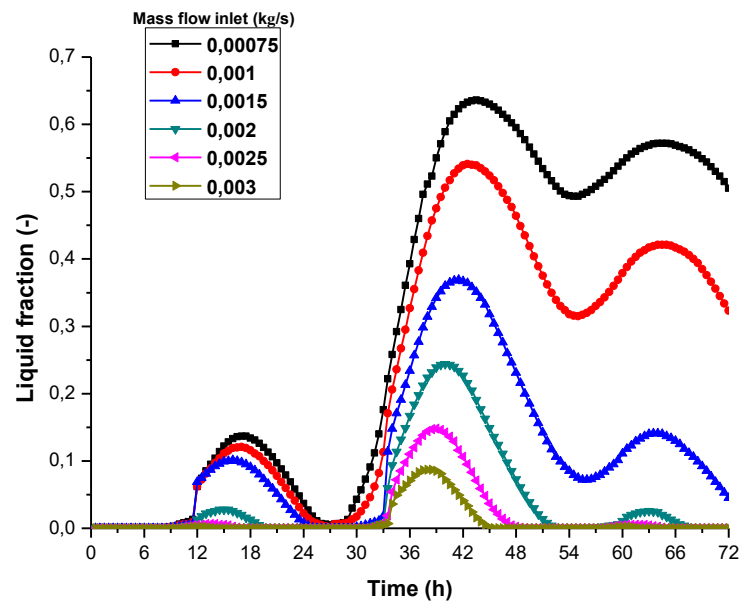
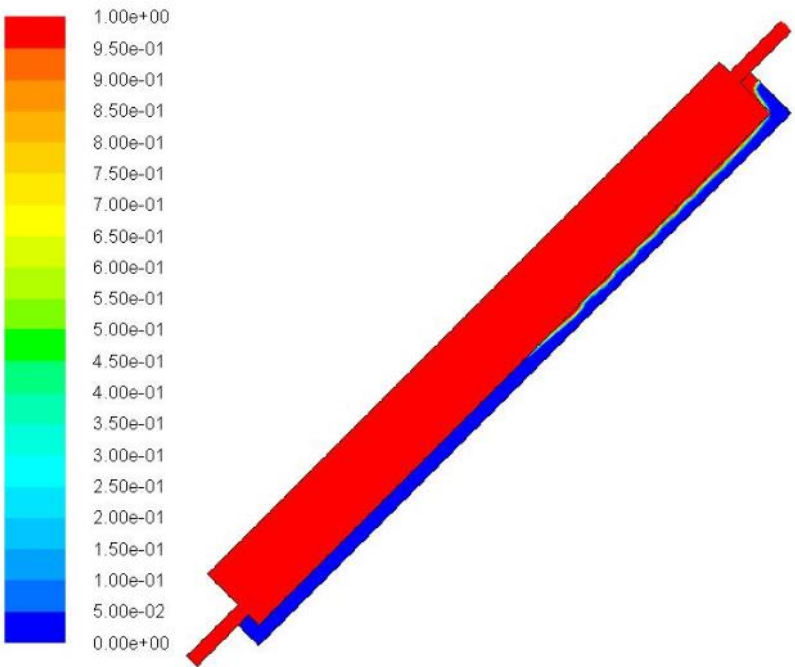
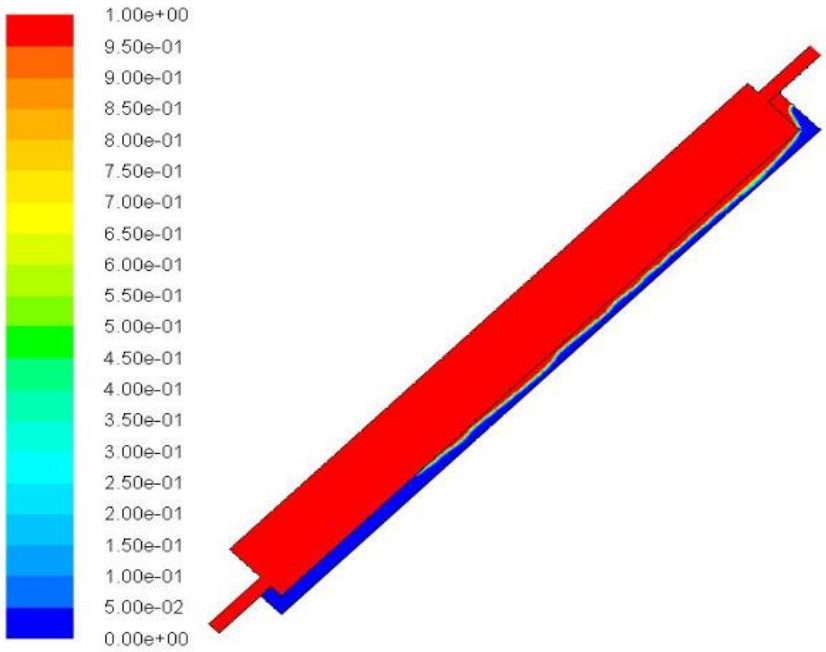


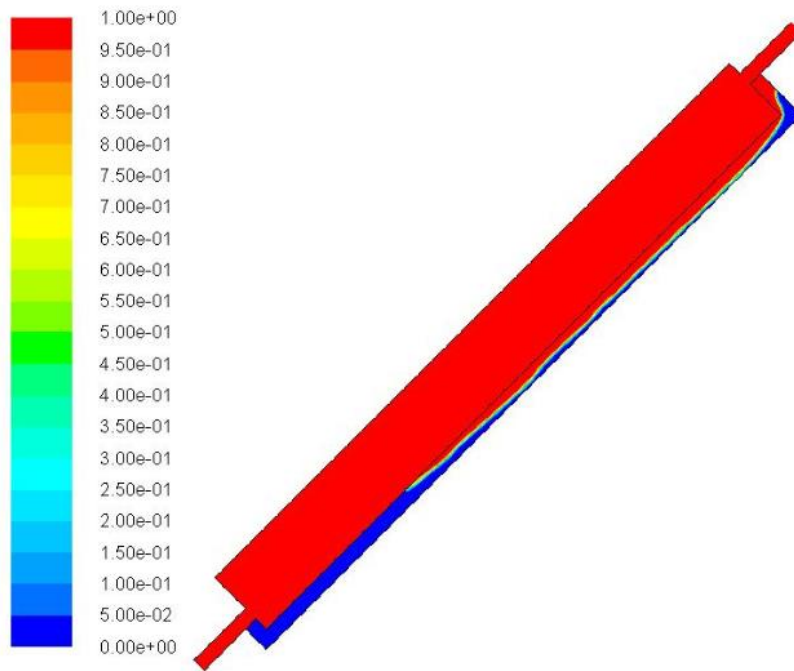
Fig. 6: Average liquid fractions of the PCM versus the time (case (b))



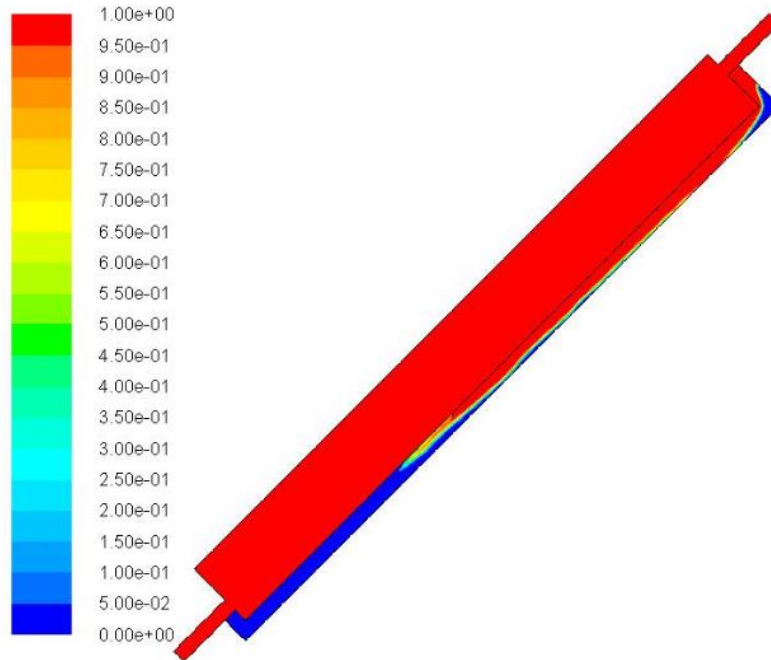
At t= 33 h



At t= 36 h

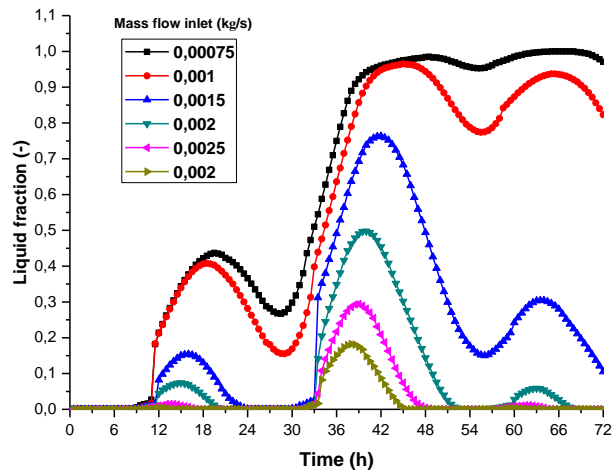


At t= 39 h

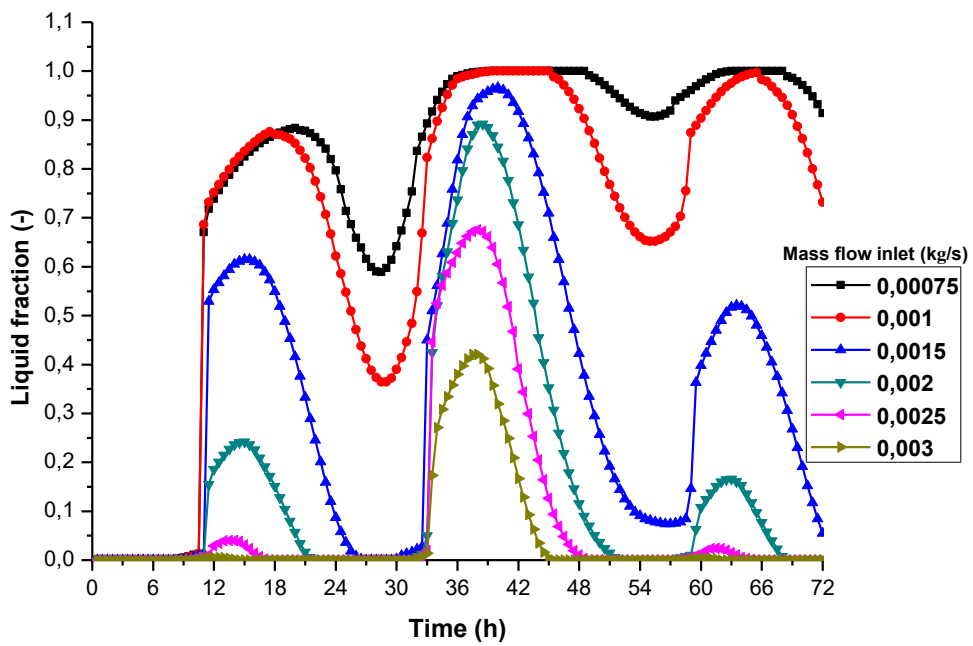


At t= 42 h

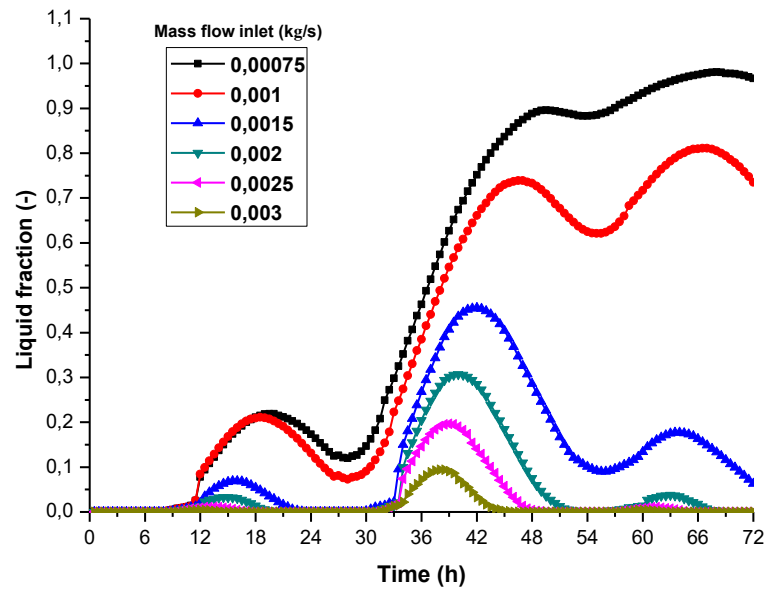
Fig. 7: Liquid fraction contours at various times from the sunrise (C1)



(a) Layer thickness=0.02 m

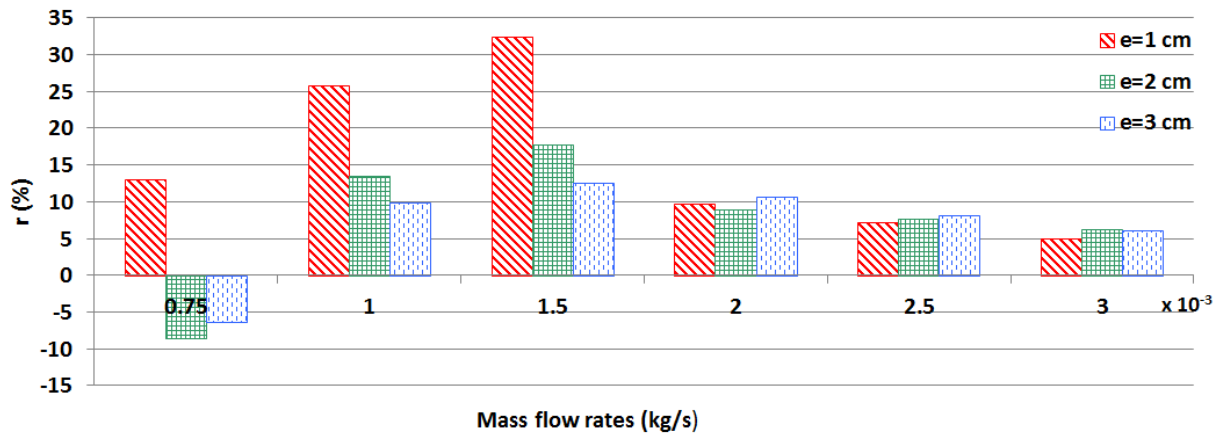


(b) Layer thickness=0.01 m

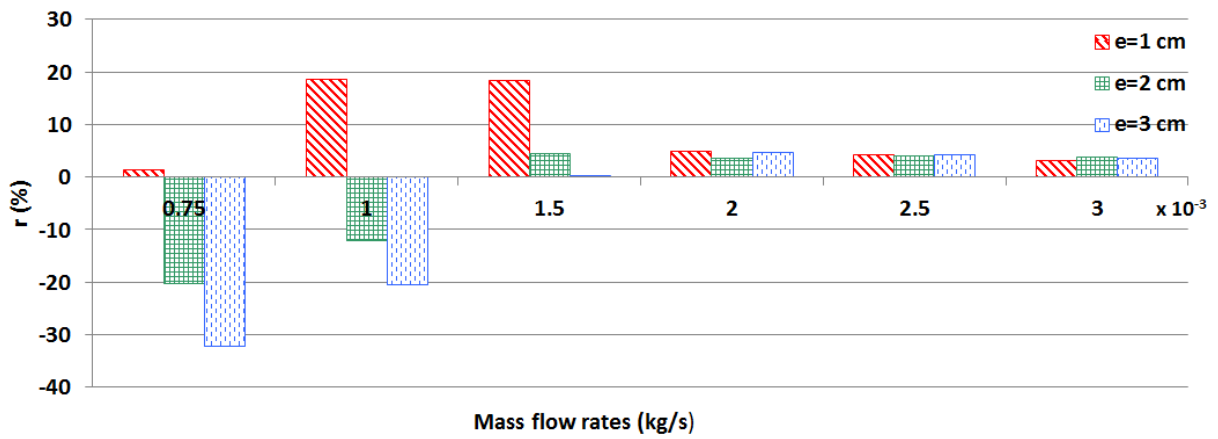


(c) Layer thickness=0.03 m

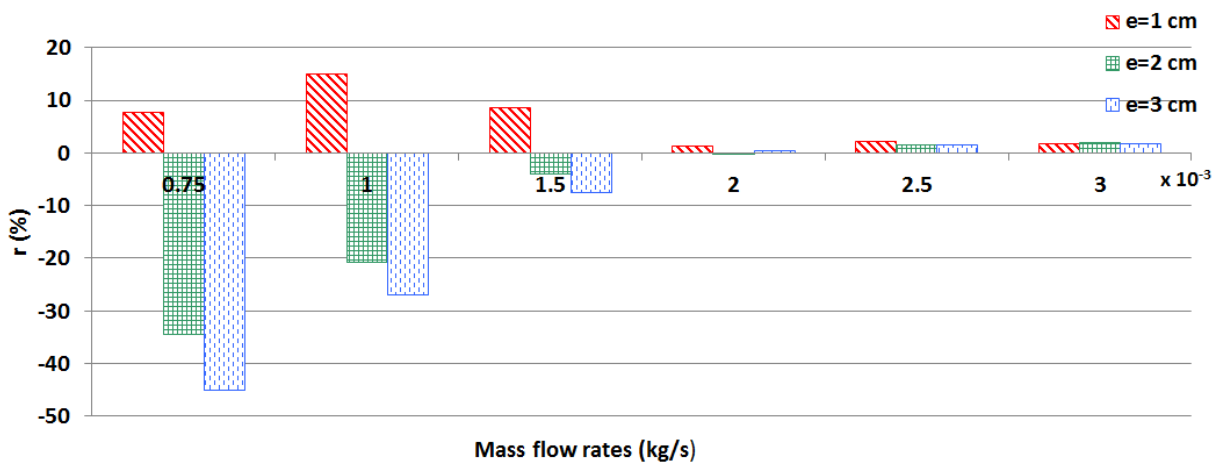
Fig. 8: Average liquid fractions of the PCM versus the time (C2)



(a) $T_{set}=313\text{ K}$



(b) $T_{set}=318\text{ K}$



(c) $T_{set}=323\text{ K}$

Fig. 9: Reduction in the daily missed thermal energy

Table 1: Thermo physical properties of the PCM (n-eicosane (C₂₀H₄₂))

Density (kg/m ³)	Liquid: 780; Solid: 820
Thermal conductivity (W/m K)	Liquid 0.16; Solid: 0.212
Dynamic viscosity (kg/m s)	3.9×10^{-3}
Specific heat (kJ/kg K)	Liquid 2.2; solid: 1.9
Latent heat (kJ/kg)	237.4
Melting temperature (K)	309.65

Table 2: Missed thermal energy (without PCM C0, with PCM C2)

Mass flow rates (kg/s)	Energy missed (kWh)			
	Without PCM	With PCM		
		e=1 cm	e=2cm	e=3 cm
0.00075	0.0624	0.0543	0.0678	0.0664
0.001	0.1077	0.0799	0.0931	0.0970
0.0015	0.5043	0.3410	0.4152	0.4408
0.002	1.2943	1.1688	1.1788	1.1573
0.0025	2.1542	1.9995	1.9881	1.9802
0.003	3.1222	2.9648	2.9298	2.9314

(a) $T_{set}=313\text{ K}$

Mass flow rates (kg/s)	Solar energy to consumer (kWh)			
	Without PCM	With PCM		
		e=1 cm	e=2cm	e=3 cm
0.00075	0.1263	0.1246	0.1518	0.1668
0.001	0.2184	0.1777	0.2446	0.2628
0.0015	0.8173	0.6674	0.7813	0.8152
0.002	1.8355	1.7442	1.7688	1.7500
0.0025	2.9195	2.7924	2.7989	2.7954
0.003	4.1310	4.0036	3.9717	3.9770

(b) $T_{set}=318\text{ K}$

Mass flow rates (kg/s)	Solar energy to consumer (kWh)			
	Without PCM	With PCM		
		e=1 cm	e=2cm	e=3 cm
0.00075	0.2315	0.2137	0.3111	0.3356
0.001	0.4053	0.3441	0.4890	0.5142
0.0015	1.2171	1.1118	1.2647	1.3079
0.002	2.4712	2.4379	2.4747	2.4619
0.0025	3.7898	3.7021	3.7316	3.7331
0.003	5.2565	5.1674	5.1457	5.1587

(c) $T_{set}=323\text{ K}$

Table 3: Extra cost evaluation

Case	Extra cost (USD)	Extra cost (%)
Case-I (0.01 m thickness)	31.5392	14.30%
Case-II (0.02 m thickness)	63.07	28.66%
Case-III (0.03 m thickness)	94.61	43%

References

1. Liu, Y., Yu, S., Zhu, Y., Wang, D., & Liu, J. (2018). Modeling, planning, application and management of energy systems for isolated areas: A review. *Renewable and Sustainable Energy Reviews*, 82, 460-470.
2. Kabir, E., Kumar, P., Kumar, S., Adelodun, A. A., & Kim, K. H. (2018). Solar energy: potential and future prospects. *Renewable and Sustainable Energy Reviews*, 82, 894-900.
3. Sampaio, P. G. V., & González, M. O. A. (2017). Photovoltaic solar energy: Conceptual framework. *Renewable and Sustainable Energy Reviews*, 74, 590-601.
4. Kalogirou, S. A., Karellas, S., Braimakis, K., Stanciu, C., & Badescu, V. (2016). Exergy analysis of solar thermal collectors and processes. *Progress in Energy and Combustion Science*, 56, 106-137.
5. Wang, Z., Yang, W., Qiu, F., Zhang, X., & Zhao, X. (2015). Solar water heating: From theory, application, marketing and research. *Renewable and Sustainable Energy Reviews*, 41, 68-84.
6. Islam, M. R., Sumathy, K., & Khan, S. U. (2013). Solar water heating systems and their market trends. *Renewable and Sustainable Energy Reviews*, 17, 1-25.
7. Mauthner, F., Weiss, W., & Spörk-Dür, M. (2016). Solar heat worldwide: markets and contribution to the energy supply 2014. International Energy Agency-Solar Heating and Cooling Program. <<https://www.iea-shc.org/>>
8. Gautam, A., Chamoli, S., Kumar, A., & Singh, S. (2017). A review on technical improvements, economic feasibility and world scenario of solar water heating system. *Renewable and Sustainable Energy Reviews*, 68, 541-562.
9. Jaisankar, S., Ananth, J., Thulasi, S., Jayasuthakar, S. T., & Sheeba, K. N. (2011). A comprehensive review on solar water heaters. *Renewable and Sustainable Energy Reviews*, 15(6), 3045-3050.
10. Singh, R., Lazarus, I. J., & Souliotis, M. (2016). Recent developments in integrated collector storage (ICS) solar water heaters: A review. *Renewable and Sustainable Energy Reviews*, 54, 270-298.
11. Nieuwoudt, M. N., & Mathews, E. H. (2005). A mobile solar water heater for rural housing in Southern Africa. *Building and Environment*, 40(9), 1217-1234.
12. Helal, O., Chaouachi, B., & Gabsi, S. (2011). Design and thermal performance of an ICS solar water heater based on three parabolic sections. *Solar Energy*, 85(10), 2421-2432.
13. Souliotis, M., Chemisana, D., Caouris, Y. G., Tripanagnostopoulos, Y. (2013). Experimental study of integrated collector storage solar water heaters. *Renewable Energy*, 50, 1083-1094.
14. Kumar, R., Rosen, M. A. (2011). Integrated collector-storage solar water heater with extended storage unit. *Applied Thermal Engineering*, 31(2), 348-354.
15. Prakash, J., Kaushik, S. C., Kumar, R., & Garg, H. P. (1994). Performance prediction for a triangular built-in-storage-type solar water heater with transparent insulation. *Energy*, 19(8), 869-877.
16. Garg, H. P., Hrishikesan, D. S., & Jha, R. (1988). System performance of built-in-storage type solar water heater with transparent insulation. *Solar & wind technology*, 5(5), 533-538.
17. Gertzos, K. P., Caouris, Y. G., & Panidis, T. (2010). Optimal design and placement of serpentine heat exchangers for indirect heat withdrawal, inside flat plate integrated collector storage solar water heaters (ICSSWH). *Renewable Energy*, 35(8), 1741-1750.

18. Tripanagnostopoulos, Y., Souliotis, M. (2004). *Integrated collector storage solar systems with asymmetric CPC reflectors*. *Renewable Energy*, 29(2), 223-248.
19. Garnier, C., Currie, J., Muneer, T. (2009). *Integrated collector storage solar water heater: temperature stratification*. *Applied Energy*, 86(9), 1465-1469.
20. Kumar, R., Rosen, M. A. (2010). *Thermal performance of integrated collector storage solar water heater with corrugated absorber surface*. *Applied Thermal Engineering*, 30(13), 1764-1768.
21. Souliotis, M., Papaefthimiou, S., Caouris, Y. G., Zacharopoulos, A., Quinlan, P., & Smyth, M. (2017). *Integrated collector storage solar water heater under partial vacuum*. *Energy*, 139, 991-1002.
22. Devanarayanan, K., & Murugavel, K. K. (2014). *Integrated collector storage solar water heater with compound parabolic concentrator—development and progress*. *Renewable and Sustainable Energy Reviews*, 39, 51-64.
23. Ziapour, B. M., Palideh, V., & Mohammadnia, A. (2014). *Study of an improved integrated collector-storage solar water heater combined with the photovoltaic cells*. *Energy Conversion and Management*, 86, 587-594.
24. Swiatek, M., Fraisse, G., & Pailha, M. (2015). *Stratification enhancement for an integrated collector storage solar water heater (ICSSWH)*. *Energy and Buildings*, 106, 35-43.
25. Souza, J. V., Fraisse, G., Pailha, M., & Xin, S. (2014). *Experimental study of a partially heated cavity of an integrated collector storage solar water heater (ICSSWH)*. *Solar Energy*, 101, 53-62.
26. Kousksou, T., Bruel, P., Jamil, A., El Rhafiki, T., Zeraouli, Y. (2014). *Energy storage: Applications and challenges*. *Solar Energy Materials and Solar Cells*, 120, 59-80.
27. Mohamed, S. A., Al-Sulaiman, F. A., Ibrahim, N. I., Zahir, M. H., Al-Ahmed, A., Saidur, R., ... & Sahin, A. Z. (2017). *A review on current status and challenges of inorganic phase change materials for thermal energy storage systems*. *Renewable and Sustainable Energy Reviews*, 70, 1072-1089
28. Dinker, A., Agarwal, M., & Agarwal, G. D. (2017). *Heat storage materials, geometry and applications: a review*. *Journal of the Energy Institute*, 90, 1-11
29. Seddegh, S., Wang, X., Henderson, A. D., & Xing, Z. (2015). *Solar domestic hot water systems using latent heat energy storage medium: a review*. *Renewable and Sustainable energy reviews*, 49, 517-533.
30. Kee, S. Y., Munusamy, Y., & Ong, K. S. (2018). *Review of Solar Water Heaters Incorporating Solid-Liquid Organic Phase Change Materials as Thermal Storage*. *Applied Thermal Engineering*, 134, 455-471
31. Mazman, M., Cabeza, L. F., Mehling, H., Nogues, M., Evliya, H., & Paksoy, H. Ö. (2009). *Utilization of phase change materials in solar domestic hot water systems*. *Renewable Energy*, 34(6), 1639-1643.
32. Mahfuz, M. H., Anisur, M. R., Kibria, M. A., Saidur, R., & Metselaar, I. H. S. C. (2014). *Performance investigation of thermal energy storage system with Phase Change Material (PCM) for solar water heating application*. *International Communications in Heat and Mass Transfer*, 57, 132-139.
33. Kousksou, T., Rhafiki, T. E., Arid, A., Schall, E., & Zeraouli, Y. (2008). *Power, efficiency, and irreversibility of latent energy systems*. *Journal of Thermophysics and Heat Transfer*, 22(2), 234-239.
34. El Qarnia, H. (2009). *Numerical analysis of a coupled solar collector latent heat storage unit using various phase change materials for heating the water*. *Energy Conversion and Management*, 50(2), 247-254.

35. Reddy, K. S. (2007). Thermal modeling of PCM-based solar integrated collector storage water heating system. *Journal of solar energy engineering*, 129(4), 458-464.
36. Eames, P. C., & Griffiths, P. W. (2006). Thermal behaviour of integrated solar collector/storage unit with 65 C phase change material. *Energy conversion and management*, 47(20), 3611-3618.
37. Chaabane, M., Mhiri, H., & Bournot, P. (2014). Thermal performance of an integrated collector storage solar water heater (ICSSWH) with phase change materials (PCM). *Energy conversion and management*, 78, 897-903.
38. Al-Kayiem, H. H., Lin, S. C. (2014). Performance evaluation of a solar water heater integrated with a PCM nanocomposite TES at various inclinations. *Solar Energy*, 109, 82-92.
39. Ali Fazilati, M., Alemrajabi, A. A. (2013). Phase change material for enhancing solar water heater, an experimental Approach. *Energy Conversion and Management*, 71, 138-145.
40. Papadimitratos, A., Sobhansarbandi, S., Pozdin, V., Zakhidov, A., Hassanipour, F. (2016). Evacuated tube solar collectors integrated with phase change materials. *Solar Energy*, 129, 10-19.
41. Kılıçkap, S., El, E., Yıldız, C. (2018). Investigation of the effect on the efficiency of phase change material placed in solar collector tank. *Thermal Science and Engineering Progress*, 5, 25-31.
42. Khan, M. M. A., Ibrahim, N. I., Mahbubul, I.M., Ali, H. M., Saidur, R., Al-Sulaiman, F.A. (2018). Evaluation of solar collector designs with integrated latent heat thermal energy storage: A review. *Solar Energy*, 166, 334-350.
43. Pandey, A.K., Hossain, M.S., Tyagi, V.V., Rahim, N. A., Selvaraj, J. A./L., Sari, Ahmet. (2018). Novel approaches and recent developments on potential applications of phase change materials in solar energy. *Renewable and Sustainable Energy Reviews*, 82, 281-323.
44. Klein, S. A. (1975). Calculation of flat-plate collector loss coefficients. *Solar energy*, 17(1), 79-80.
45. Pirasaci, T., Wickramaratne, C., Moloney, F., Goswami, D. Y., & Stefanakos, E. (2017). Dynamics of phase change in a vertical PCM capsule in the presence of radiation at high temperatures. *Applied Energy*, 206, 498-506.
46. Kousksou, T., Mahdaoui, M., Ahmed, A., & Msaad, A. A. (2014). Melting over a wavy surface in a rectangular cavity heated from below. *Energy*, 64, 212-219.
47. Zennouhi, H., Benomar, W., Kousksou, T., Msaad, A. A., Allouhi, A., Mahdaoui, M., & El Rhafiki, T. (2017). Effect of inclination angle on the melting process of phase change material. *Case Studies in Thermal Engineering*, 9, 47-54.
48. Gau, C., & Viskanta, R. (1986). Melting and solidification of a pure metal on a vertical wall. *Journal of Heat Transfer*, 108(1), 174-181.
49. Kousksou, T., Mahdaoui, M., Hlimi, M., El Alaiji, R., & El Rhafiki, T. (2016). Latent energy storage: Melting process around heating cylinders. *Case Studies in Thermal Engineering*, 8, 128-140.
50. Ho, C. J., Huang, J. B., Tsai, P. S., & Yang, Y. M. (2011). Water-based suspensions of Al₂O₃ nanoparticles and MEPCM particles on convection effectiveness in a circular tube. *International Journal of Thermal Sciences*, 50(5), 736-748.